International Conference on Estuaries and Coasts
November 9-11, 2003, Hangzhou, China

MODELLING THE FLOW IN CURVED TIDAL CHANNELS AND RIVERS

Robert BOOIJ
Faculty of Civil Engineering and Geosciences, Delft University of Technology,
P.O. Box 5048, 2600 GA Delft, The Netherlands. Tel.: +31 (0)15 278 45 82;
Fax: +31 (0)15 278 59 75 E-mail: r.booij@citg.tudelft.nl

Abstract: Flows in tidal channel bends and river bends are very shallow and mildly curved free surface flows. The shallowness and the curvature of the flow lead to a few flow features which are difficult to reproduce with numerical models. An example is the second counter-rotating secondary flow cell that is observed along steep outer banks in river bends. This second cell has important consequences for the undermining of the outer bank. Only in relatively deep flows RANS-models do succeed in reproducing this second cell.
Understandably the shallowness of this kind of flows leads to a preference for 2-D horizontal models. However, it is well known that due to differential advection main flow momentum is advected from the region of low velocity at the inside bend to the region with high velocity near the outside bend. Thus a negative eddy viscosity is required in a 2-D model, which however leads to stability problems. In 3-D computations there is no problem as the secondary flow and its advection effects are included in the computation.
In curved shallow free surface flow another negative eddy viscosity phenomenon was observed, however. If the shear stress component that transports main flow across the channel is expressed as a gradient type of momentum transport, then again a negative eddy viscosity appears. This means that 3-D computations with gradient type turbulence models (e.g. eddy viscosity or k-ε models) can never yield such a stress component with the correct sign. The negative eddy viscosity can be understood by looking at the mechanism that creates the shear stresses, in this case parcels of water that move upwards and downwards over the flow retaining a substantial part of their original momentum. If we describe the exchange of momentum with a kind of vertical mixing length model, the same mixing length leads to correct shear stresses for all three stress components. In contradistinction to gradient type turbulence models, large eddy simulation (LES) does yield correct shear stresses.

Key words: River bends, tidal channel bends, Shallow flow, Free surface flow, Secondary flow, Counter-rotating cell, Negative eddy viscosity, Mixing length, Turbulence models, RANS, LES.

1. INTRODUCTION

Many flows of interest in environmental fluid mechanics, e.g. flows in channels, rivers, lakes, estuaries and seas, are shallow turbulent free surface flows. In these flows the important horizontal length scales of the flow are one or more orders of magnitude larger than the flow depth. For example, tidal channel bends and river bends have large aspect ratios $\{W/h \geq O(50)\}$ and curvature ratios $\{R/h \geq O(50)\}$ generally, where h, W and R are the depth, width and radius of curvature respectively. In laboratory models these large ratios are not feasible in most cases. Often the models used are hardly shallow (e.g. models of meandering rivers with aspect ratios of 2 to 4), see figure 1. This leads to a defective modelling of the shallow flow and/or a very restricted insight in the physical processes in shallow flow (Booij, 2003a). The shallowness of most environmental flows complicates their numerical reproduction. An example is the second, counter-rotating, secondary flow cell in river bends

and tidal channel bends, see Fig. 2 (Vriend, 1981). For relatively deep laboratory model flows this second cell is easy to reproduce with Reynolds average numerical simulations (RANS), but not in real shallow flow situations (Booij, 2003b).

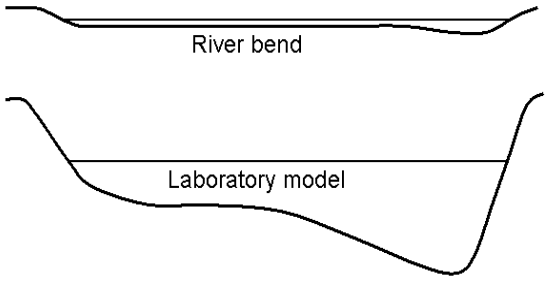

Fig. 1 Cross-section of a shallow river bend and its usual deep laboratory model

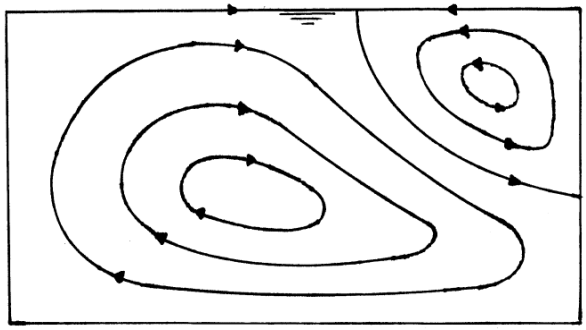

Fig. 2 Sketch of two cell system of the second-ary flow in a river bend with steep outside bank

The largest flow velocities in mildly curved shallow free surface flow are found at the outside of the curved flow, e.g. the outer bend in curved river flow. The mechanism that makes the flow velocity at the outside of the curvature increase at the expense of the velocity at the inside is differential advection, which can be understood as follows. In mildly curved shallow flow the main flow velocity profile over the vertical is almost logarithmic. Hence the centrifugal force due to the curvature of the flow is larger in the upper part of the flow than near the bottom. On the average this centrifugal force is comp ensated by the pressure gradient due to a surface slope towards the outer bend. The resulting force is directed to the outward side in the upper part of the flow and to the inward side near the bottom and hence leads to a secondary flow to the outside in the upper part and to the inside near the bottom (see Fig. 3). The main flow and the secondary flow together form the helical flow observed in curved shallow flow. In mildly curved shallow flow the amount of water flowing outward is more or less equal to the amount of water flowing inward. However the main flow velocity is larger in the upper part of the flow than in the lower part, hence more main flow momentum is transported outwards in the upper part of the flow than inwards in the lower part. This leads to a net transport of main flow momentum in outward direction and consequently to higher flow velocities at the outer bend.

In view of the shallowness of rivers and tidal channels the preference for 2-D horizontal models is understandable. However, the momentum transport by differential advection (i.e. from the region of low velocity at the inside bend to the region with high velocity near the outside bend) requires the implementation of a negative eddy viscosity, which will lead to stability problems. In 3-D computations the secondary flow is computed and hence its advection effects are included, without the necessity of a negative eddy viscosity.

Extensive measurements of main flow and turbulent stresses in a model of a curved shallow free surface flow (Booij and Tukker, 1996) showed another negative eddy viscosity

phenomenon. If the shear stress component that transports main flow across the channel is expressed as a gradient type of momentum transport, then again a negative eddy viscosity appears. This negative eddy viscosity and a discussion of the mechanism of momentum transport that explains this negative eddy viscosity form the main subject of this paper.

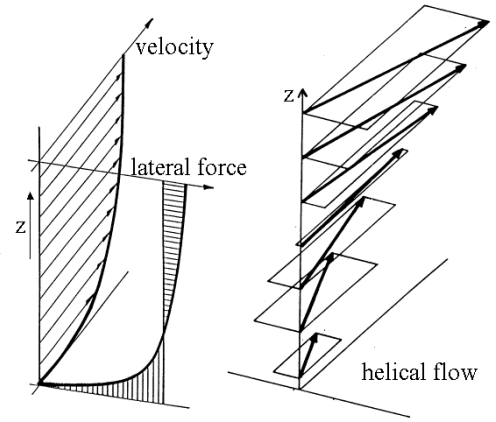

Fig. 3 Mechanism of differential advection

EXPERIMENTAL SETUP

The measurements discussed in this paper were obtained in the curved flume of the Laboratory for Fluid Mechanics of Delft University of Technology (DUT) (see Fig. 4). The flume is a compromise between real river bends and the possibilities in a laboratory. The cross-section of the flume is rectangular and the measures of the flume are $h = 52$ mm, $W = .50$ m and $R = 4.10$ m. Hence the flume is a model of a relatively shallow ($W/h \approx 10$) and mildly curved river bend ($R/h \approx 80$). An advantage of this layout is that the flow becomes almost uniform in the second part of the bend (> 90º), which makes the flow more appropriate for theoretical investigation and validation of numerical models. A flow of about 5.2 l/s was used, corresponding to an average velocity of about 0.2 m/s over the cross-section.

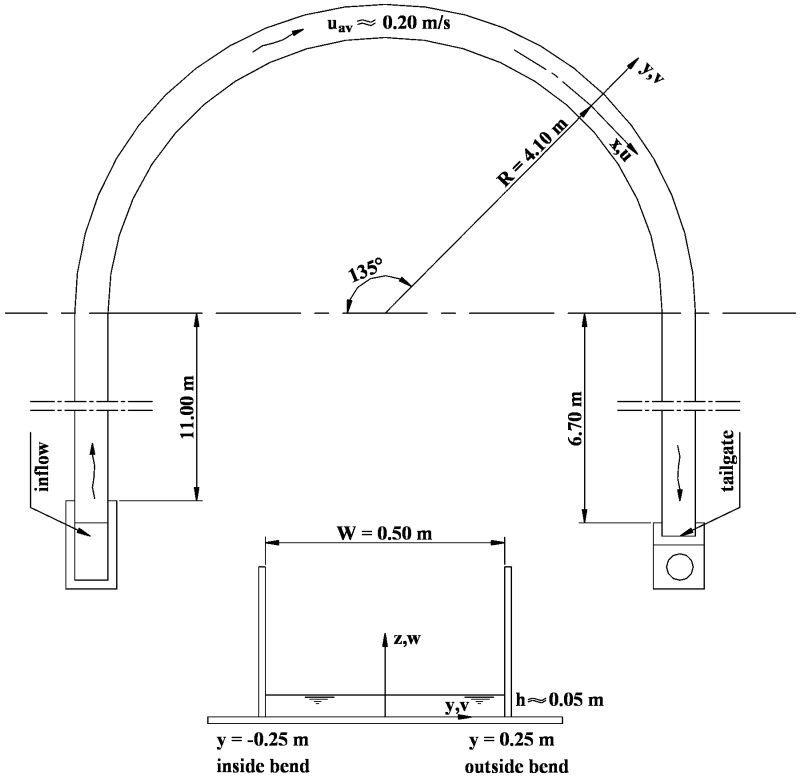

Fig. 4 The curved flume of Delft University of Technology (top view and cross-section)

All measurements discussed here were executed in the nearly uniform flow region at the cross-section of 135º with a 3D laser Doppler velocity (LDV) system, measuring through the glass bottom of the flume. The measurements were executed with a DANTEC 3-colour fibre optics system with a 4-Watt Coherent Ar-ion laser and DANTEC BSA processors. The optical system used was a combination of a 2-dimensional probe and a 1-dimensional probe, see Fig. 5. The velocity components measured with the 2-D probe (directions 2 and 1 in Fig. 5) are the velocity component in transverse direction v and a combination of tangential and vertical velocity components u and w. Combination of the last one with the velocity component (direction 3 in Fig. 5) measured with the 1-D probe yields u and w. The relatively large angle (60˚) between directions 1 and 3 allows for a relatively precise determination of w with this beam configuration. Identity of the measured particles is assured by requiring arrival time coincidence.

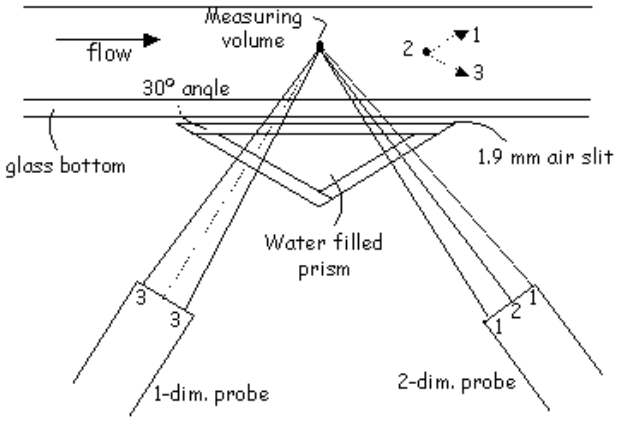

Fig. 5 The 3-dim. LDV beam configuration

To simplify aligning of the many laser beams a water-filled prism, with sides perpendicular to the optical axes of the two probes, was attached under the measuring cross-section , see Fig. 8. The refraction by the glass-plates forming the bottom of the flume and the top of the prism, which were at an angle to the optical axis, complicated the creation of overlapping measuring volumes for the different beam pairs. This refraction effect of the glass plates could be effectively compensated for by a small air-filled slit between them. The measuring system can be traversed in y- and z-direction and the two probes independently in the x-direction. This combination of 4 movements is required to be able to execute measurements over the cross-section without having to align the beams between measurements. A small measuring volume of the order of 1 mm in all three directions was realized. The measuring time in each point was 6 minutes. .

2. SECOND COUNTER-ROTATING SECONDARY FLOW CELL

The measurements clearly showed the existence of a counter-rotating secondary flow cell along the outer bank (see Fig. 6), which was earlier mainly reported from measurements in the complete cross-section, the outside part (blown up for clarity). relatively deep and sharply curved flumes (Blanckaert and Graf, 1999).

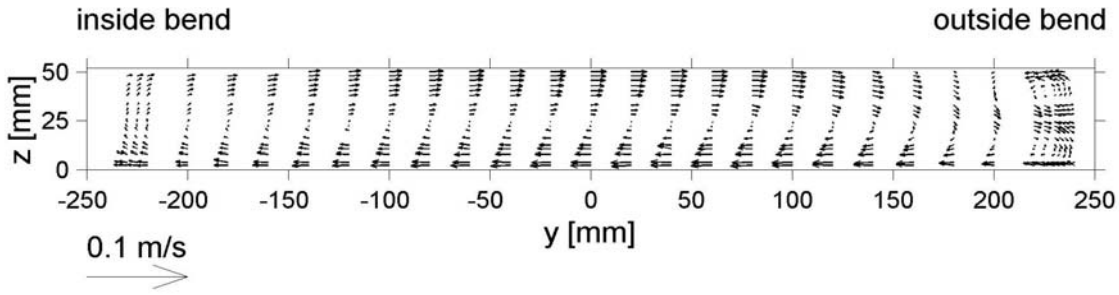

a)

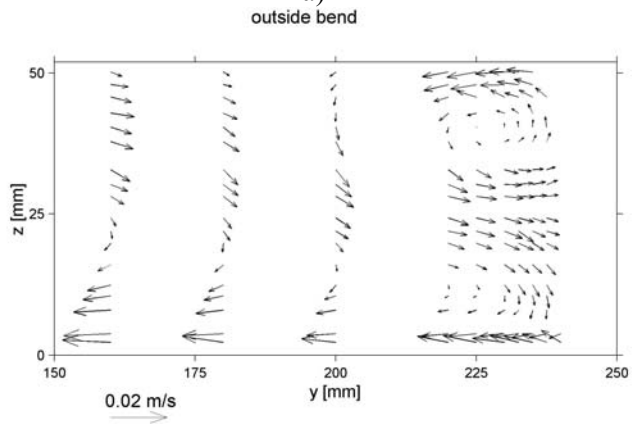

b)

Fig. 6 Measured secondary flow field, showing a counter-rotating cell along the upper outside wall

Standard RANS models can reproduce the main characteristics of the main flow and of the secondary flow patterns. However, the reproduction of the second, counter-rotating, cell depends on the sharpness of the bend. In sharp river bends (R/h<20) it is relatively easy to compute this second cell with several RANS models. However for more realistic gentle bends (R/h>50) the second cell is not reproduced (see Booij, 2003a). In Fig. 7a the result of a computation of the flow in the DUT-flume with a k-ε model is shown. The counter-rotating shell is not reproduced. A 3-D large eddy simulation (LES) computation did succeed in reproducing the second cell (see Fig. 7b) in spite of the for LES unfavourable aspect ratio W/h ≈ 10 of the flume (Booij, 2002). However, 3-D LES is not yet applicable for the computation of more realistic river layouts.

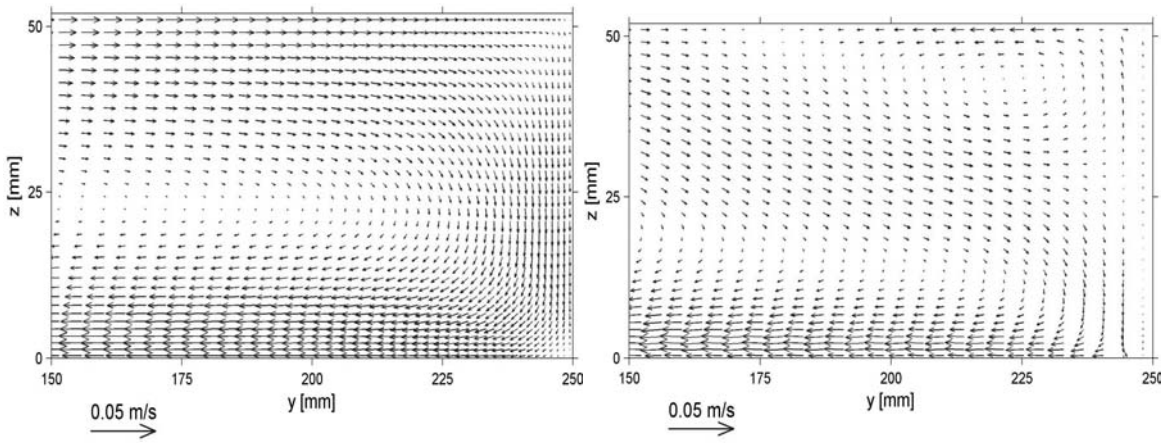

a) k-ε, model b) LES

Fig. 7 The computed secondary flow field in the outside part of the cross-section at 135°
a) k-ε model; b) LES computation, showing the counter-rotating cell along the upper outside wall

NEGATIVE EDDY VISCOSITY

In figure 8 the measured time-averaged velocity profiles and shear stress profiles in the centre of the cross-section are plotted. Remarkable is the positive value of the shear stress $\tau_{xy} = \rho\overline{u'v'}$ over the lower half of the vertical, which shear stress transports main flow momentum across the flume. If gradient-type momentum transport is assumed for the different shear stresses, values for the related eddy viscosities can be obtained using the following relations:

$$\frac{\tau_{xz}}{\rho} = \overline{u'w'} = -\nu_{xz}\left(\frac{\partial U}{\partial z} + \frac{\partial W}{\partial x}\right) = -\nu_{xz}\frac{\partial U}{\partial z}$$

$$\frac{\tau_{xy}}{\rho} = \overline{u'v'} = -\nu_{xy}\left(\frac{\partial U}{\partial y} + \frac{\partial V}{\partial x}\right) = -\nu_{xy}\left(\frac{\partial U}{\partial y} - \frac{U}{R}\right)$$

$$\frac{\tau_{yz}}{\rho} = \overline{v'w'} = -\nu_{yz}\left(\frac{\partial V}{\partial z} + \frac{\partial W}{\partial y}\right) = -\nu_{yz}\frac{\partial V}{\partial z}$$

where the used approximations are allowed (but not too close to the sidewalls) because of the uniform flow in this section of the flume. The obtained values for the eddy viscosities are plotted in Fig. 9. Related to the positive value of τ_{xy} is the negative value of the corresponding eddy viscosity ν_{xy}. This negative eddy viscosity applies for a large part of the cross-section (see Fig. 10). For comparison the theoretical parabolic eddy viscosity profile for wide straight uniform flow $\nu_{xz} = \kappa u_* z(1 - z/h)$ with $\kappa = 0.4$ (corresponding to a logarithmic velocity profile) is included in the plot of figure 9. As curvature is assumed to suppress this vertical momentum exchange, another profile with lower κ (=0.3) is added. Because gradient type momentum transport models require positive eddy viscosities, the negative value obtained from the measurements explains the inability of this kind of models to reproduce correct shear stresses (see Fig. 11(top) for a k-ε model), in contradistinction to the cor- rect shear stresses computed with LES (see Fig. 11(bottom)).

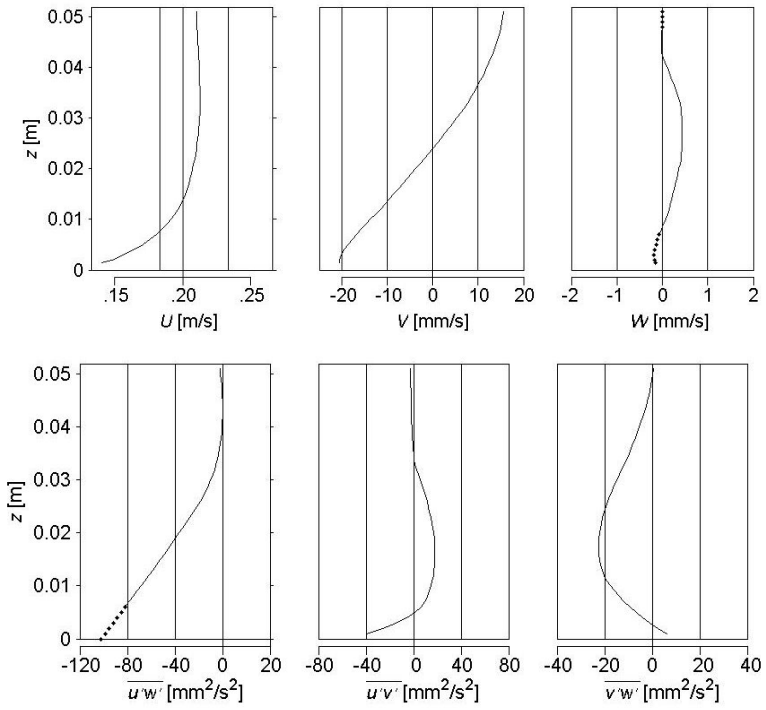

Fig. 8 Vertical profiles of the measured time- averaged velocity components (top) and shear stresses (bottom). (= approximate and/or extrapolated part of the vertical)

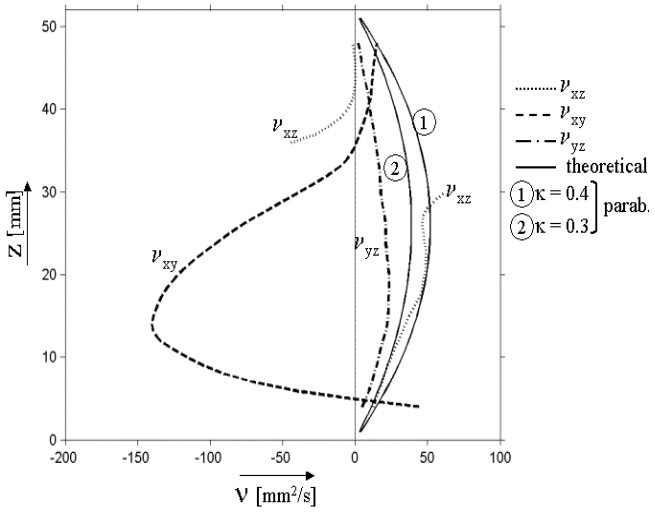

Fig. 9 Eddy viscosity profiles corresponding to the three shear stresses τ_{xz} , τ_{xy}, and τ_{yz} compared to theoretical parabolic profiles

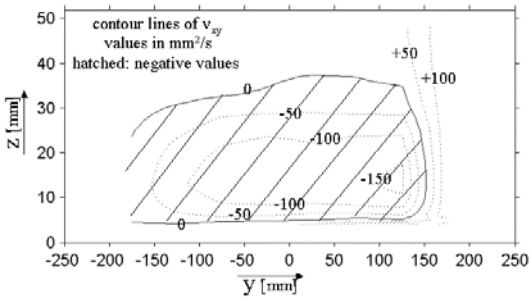

Fig. 10 Part of cross-section with negative ν_{xy} values

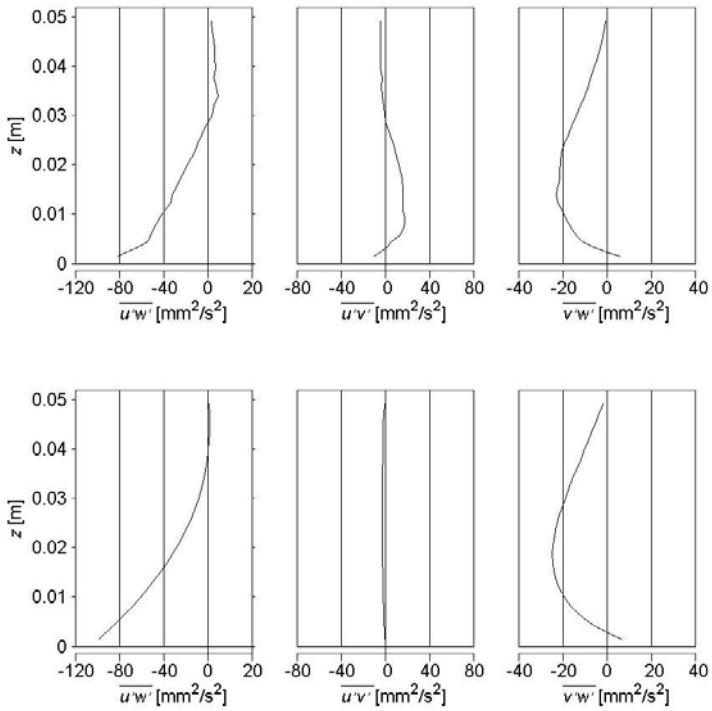

Fig. 11 Computed shear stress profiles. Top: k-ε model; bottom: LES computation

EXTENDED MIXING LENGTH CONCEPT

The sign of the shear stresses can be understood if a totally different mechanism is assumed to be responsible for the turbulent velocities in this part of the flow. Parcels of water that move upward from near the bottom arrive at a higher level in the fluid with a positive value of w and relatively low values of u and v, implying a positive w' and negative u' and v'. Downward moving parcels have analogously a negative w' and positive u' and v'. Both kind of parcels give a negative contribution to $\overline{u'w'}$ and $\overline{v'w'}$ but a positive contribution to $\overline{u'v'}$. The positive value of $\overline{u'v'}$ has then evidently nothing to do with a gradient of U across the flume as is basic in the gradient type transport theory.

This idea can be worked out using an extension of the mixing length theory of Prandtl. Turbulent parcels of water that move upward through a certain level are assumed to originate from an average distance l_m, the mixing length, below this level. They have consequently a slightly different velocity, fitting to the level of origin of the parcel, which deviation can be estimated by $u' = -l_m \partial U/\partial z$ and $v' = -l_m \partial V/\partial z$. The vertical velocity component w' is positive and is generally assumed to have roughly the same magnitude as u' so $w' = l_m \left|\partial U/\partial z\right|$. A parcel going downward has correspondingly $u' = l_m \partial U/\partial z$, $v' = l_m \partial V/\partial z$ and $w' = -l_m \left|\partial U/\partial z\right|$. Averaging over all particles in this model yields consequently

$$\frac{\tau_{xz}}{\rho} = \overline{u'w'} = -l_m^2 \left|\frac{\partial U}{\partial z}\right| \frac{\partial U}{\partial z}$$

$$\frac{\tau_{xy}}{\rho} = \overline{u'v'} = +l_m^2 \frac{\partial U}{\partial z} \frac{\partial V}{\partial z}$$

$$\frac{\tau_{yz}}{\rho} = \overline{v'w'} = -l_m^2 \left|\frac{\partial U}{\partial z}\right| \frac{\partial V}{\partial z}$$

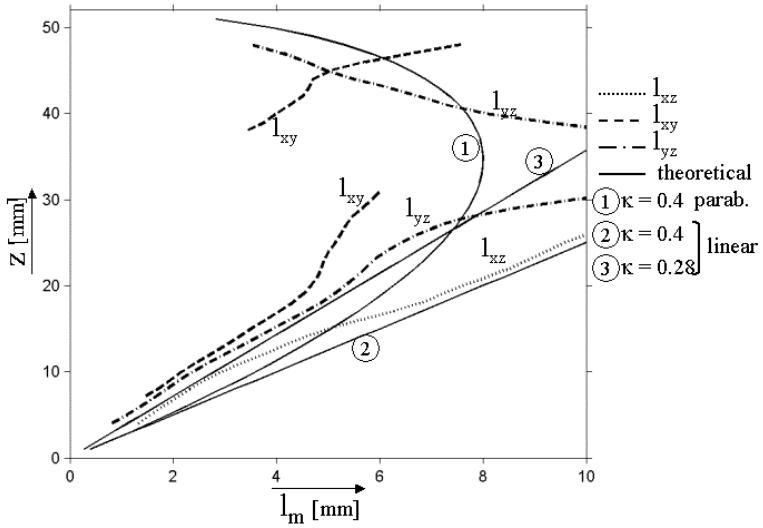

Fig. 12 Mixing lengths corresponding to the three measured shear stresses in the center of the flume

This concept can be evaluated by inspection of the values of l_m obtained from the three measured shear stresses and the gradients of the time-averaged velocity components, see Fig. 12. Here the mixing length obtained from the measured shear stress τ_{xz} is notated l_{xz}, etc. The three mixing lengths are compared in Fig. 12 with the theoretical

Bakhmetev distribution $l_m = \kappa z\sqrt{(1-z/h)}$, which applies for a straight, wide and uniform free surface flow when a logarithmic velocity profile (with $\kappa = 0.4$) and a linear shear stress distribution are assumed. In the upper part of the flow the time-averaged velocity and the shear stresses deviate strongly from those in a straight flume because of the curvature of the flow. Moreover the velocity gradients and shear stresses are small in that region. Therefore the mixing lengths in the upper half of the flow can hardly be determined. In the lower half the three mixing lengths are all of the same order of magnitude. Moreover they compare well to the Bakhmetev distribution, or the linear distribution expected in the near wall region (see Fig 12), especially if again a slightly lower value of κ (= 0.28) because of the suppression of the turbulence due to the curvature is assumed.

The agreement between the different measured mixing lengths for the three shear stresses corroborates the extended mixing length concept. It may be a promising tool for other flows with large velocity gradients over the depth and a strongly depth-depending flow direction. In LES computations the movement of fluid parcels itself is computed, which explains the good result of the LES computation for all shear stresses.

3. CONCLUSIONS

- The shallow curved free surface flows in tidal channels and river bends show certain flow features that are difficult to model numerically.
- RANS (e.g. k-ε model) computations can produce the main characteristics of the main flow and the secondary flow in curved tidal channels and rivers. However, they fail to give satisfactory reproductions of some flow features, e.g. the second counter-rotating secondary flow cell and shear stresses of the proper sign.
- 3-D LES correctly reproduces the shear stresses and other flow aspects, but is not yet applicable for the computation of more realistic river layouts.
- An extended vertical mixing length model appears to be promising for flows with a depth-dependent flow direction as above the bed in tidal channel and river bends.

ACKNOWLEDGEMENTS

The author thanks J. Tukker for the accurate execution of the measurements,

REFERENCES

Blanckaert, K. and Graf W.H., 1999, "*Outer-bank cell of secondary circulation and boundary shear stress in open-channel bends"*, Proceedings of the 1st RCEM symposium, **I** 533-543, Genova, Italy.

Booij, R., 2002, "*Modelling of the secondary flow structure in river bends*", Proceedings of the International Conference on Fluvial Hydraulics, I 127-133, Louvain-la Neuve, Belgium.

Booij, R., 2003a, "*Laboratory experiments of shallow free surface flows*", Proceedings of the International Symposium on Shallow Flows, I 101-108, Delft, The Netherlands.

Booij, R., 2003b, "Measurements and large eddy simulation of flows in some curved flumes", Journal of Turbulence, 4 (2003) 008.

Booij, R. and Tukker J., 1996, "*3-Dimensional laser Doppler measurements in a curved flume*", in "*Developments in Laser Techniques and Applications to Fluid Mechanics*", Eds. R.J. Adrian, et al., 98-114, Springer, Berlin.

Vriend, H.J. de, 1981, "*Velocity redistribution in curved rectangular channels",* Journal of Fluid Mechanics, **107,** 423-439.